Spin freezing process in a reentrant ferromagnet studied by neutron depolarization analysis

T. Sato, T. Shinohara, and T. Ogawa
Department of Applied Physics and Physico-Informatics, Faculty of Science and Technology, Keio University, 3-14-1 Hiyoshi, Kohoku-ku, Yokohama-shi, Kanagawa 223-8522, Japan

M. Takeda*
Physics Department, Graduate School of Science, Tohoku University, Sendai 980-8578, Japan
(Received 29 March 2004; published 15 October 2004)

The spin freezing process and the magnetic nature of reentrant spin-glass (RSG) and the ferromagnetic (FM) phases of a typical reentrant ferromagnet $Ni_{78}Mn_{22}$ were investigated based on neutron depolarization analysis, and the results were compared with the previous Mössbauer measurements [Phys. Rev. B **64**, 184432 (2001)]. The wavelength-dependent polarization, under a field cooled (FC) condition, showed the damped oscillatory behavior in both the RSG and FM phases, except in the temperature region just above the RSG temperature $T_{RSG} \sim 60$ K. At a temperature of around 80 K, however, it showed a double oscillatory behavior. The field integral I, which is proportional to the mean local magnetic induction, was deduced as a function of the temperature. Two branches of temperature-dependent field integrals were found: a low-temperature I_{low}-branch, which has a small value of I, stopped at a temperature below the Curie temperature $T_C \sim 160$ K, and a high temperature I_{high}-branch, which has a large value of I, appeared just below 80 K. This means that there are two kinds of magnetic environments, and they have different values of magnetization. This is consistent with the observation of the double peak spectrum of the hyperfine field in the previous Mössbauer measurements. The present neutron data and the Mössbauer data can be interpreted along a scenario of reentrant behavior, which consists of the low-temperature spin canting state and the "melting of frustrated spins" mechanism introduced by Saslow and Parker [Phys. Rev. Lett. **56**, 1074 (1986)], except for the absence of the observation of singularity in the temperature-dependent magnetization. Based on such considerations, we constructed a comprehensive picture of the spin freezing process and the magnetic nature of the RSG and FM phases in the reentrant ferromagnet.

DOI: 10.1103/PhysRevB.70.134410 PACS number(s): 75.50.Lk, 75.30.Kz, 61.12.Ex

I. INTRODUCTION

Reentrant ferromagnets undergo a transition from a paramagnetic to a ferromagnetic (FM) phase as the temperature is lowered, and at lower temperatures, further transition to a state known as reentrant spin-glass (RSG) occurs.[1] This kind of successive magnetic transition has been qualitatively understood on the basis of the mean-field picture, i.e., the Sherrington-Kirkpatrick model for the Ising spin system,[2] or the model for the Heisenberg spin system introduced by Gabay and Toulouse.[3] Despite this understanding, some aspects of the intrinsic nature of reentrant ferromagnets remain to be clarified, i.e., the magnetic nature of the FM and RSG phases, and the spin-freezing process from the ordered phase to the disordered phase. The mean-field theories have predicted the existence of a low-temperature "mixed" state below a certain temperature in the ferromagnetic phase.[2,3] This is consistent with the observation, based on neutron depolarization analysis, of long range ferromagnetic correlation in the RSG phase.[4] However, some studies of neutron scattering[5] and the dynamic behavior of magnetic susceptibility[6,7] indicate an equilibrium transition from the ferromagnetic to the pure spin-glass phase. In addition, the FM phase of the reentrant ferromagnet shows peculiar behavior that reflects the chaotic nature of this phase,[8] in contrast to the robust nature of the regular ferromagnetic phase. These characteristics, observed in the RSG and FM phases, have not been sufficiently interpreted based on the mean-field model. This ambiguity makes it difficult to understand the spin freezing process in a reentrant ferromagnet.

In our previous study, mainly using the ac-susceptibility and Mössbauer techniques, we examined the intrinsic properties of the RSG transition in ^{57}Fe-doped NiMn ($Ni_{77}{}^{57}Fe_1Mn_{22}$).[9] The most remarkable feature was that the distribution of the hyperfine field in the zero-field Mössbauer data consisted of two peaks in the FM phase, and of one antisymmetric peak in the RSG phase. Based on this finding, we proposed the following picture of spin freezing in the reentrant NiMn. In the FM phase, there are two groups of spins with different relaxation times; one consists of spins, with a shorter relaxation time, around a frustrated spin site on which the spin is melting, the other of collinear spins with a longer relaxation time. Upon lowering of the temperature, the spin-glass correlation develops at the expense of spins that have faster dynamics, and then diverges at the RSG transition temperature. This kind of spin freezing process is reminiscent of the reentrant behavior driven by the mechanism of "melting of frustrated spins" introduced by Saslow and Parker.[10] It is the purpose of this paper to discuss the spin freezing of a typical reentrant ferromagnet $Ni_{78}Mn_{22}$ based on complementary information provided via a technique that has a spatial resolution different from the spatial resolution in the Mössbauer effect, which has an atomic scale resolution and a magnetic measurement on a macroscopic scale, which was used in the previous study.

The neutron depolarization analysis is a useful method to obtain information on a scale larger than 10^3 angstroms.[11] Previous neutron depolarization analysis of reentrant ferromagnet $Ni_{77}Mn_{23}$ showed characteristics suggesting the existence of a ferromagnetic domain in the RSG phase.[4,12] As a result, the low temperature irreversible magnetic behavior in NiMn reentrant ferromagnet has been interpreted in terms of the magnetic domain wall motion and the dynamics of magnetization in each domain. This is consistent with the domain-anisotropy model, which has provided a macroscopic explanation of the magnetic behavior of the NiMn system.[13] In addition, we found that the field integral, proportional to the amplitude of mean local magnetic induction in the magnetic medium, showed a two-stage increase as the temperature was lowered; i.e., the gradient of the temperature-dependent field integral significantly changed around the reentrant spin-glass temperature T_{RSG}.[12] This feature contrasts with the observation of the field integral in conventional reentrant ferromagnets, in which it shows a broad peak around T_{RSG} and successively shows a slow drop at lower temperatures.[14] This kind of singular change in NiMn reentrant ferromagnet must appear on a semimacroscopic scale, which is smaller than the spatial scale related to the dynamics of domain wall and intradomain magnetization. It is, therefore, hoped that examination of the characteristic behavior of the field integral, in relation to observation of the double distribution of the hyperfine field, can throw light on the spin freezing mechanism in a reentrant ferromagnet.

In this work, the neutron depolarization analysis of a reentrant ferromagnet $Ni_{78}Mn_{22}$, which had the same Mn concentration as that used in the previous Mössbauer measurement, was carefully performed as a function of the neutron wavelength λ with a higher resolution than that used previously. A sample consisting of a mirror-polished disk that was thinner than that used in the previous neutron depolarization measurement was used in order to observe the detailed structure of the wavelength-dependent polarization. As a result, we found two branches in the temperature-dependent field integral above T_{RSG}, which is analogous to the thermal evolution of the hyperfine field in the Mössbauer measurement. This was just as expected, given the mechanism of "frustrated-spin melting" in the spin freezing process.[10] Thus, the neutron depolarization data strongly supports our characterization of the reentrant behavior deduced from the Mössbauer measurement. After all, the change in the spin configuration was consistently characterized at various temperatures. Finally, we constructed a comprehensive picture of the spin freezing process and the magnetic nature of the RSG and FM phases in a NiMn reentrant ferromagnet.

II. EXPERIMENTAL PROCEDURE AND MAGNETIC CHARACTERIZATION

The procedure for preparing the $Ni_{78}Mn_{22}$ was similar to that for the $Ni_{77}Mn_{23}$:[12] Ni and Mn were arc-melted together under argon in the desired composition, and the ingot was homogenized for three days at 900 °C and then quenched in water. A plate of sample 0.825 ± 0.005 mm in thickness was cut from the ingot for the neutron measurement. A spherical sample ~1 mm in diameter and a small disc sample, having the same demagnetization factor as that of the neutron sample, were used for the magnetic measurements.

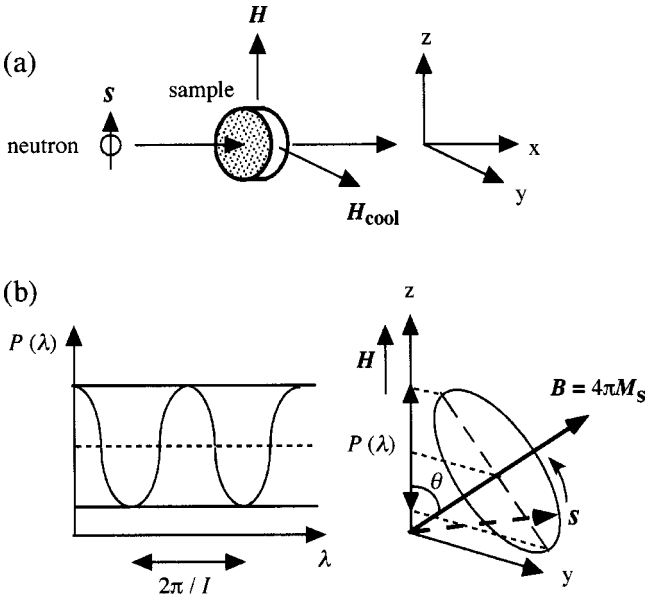

FIG. 1. The geometry of the neutron experiment is shown in (a). The neutron passes through the sample along the *x* direction, where the sample plate is parallel to the *yz* plane. The magnetic field is applied along the *z* direction. Under the FC condition, the magnetic field H_{cool} is applied along the *y* direction during the sample cooling procedure. As shown in (b), the neutron polarization shows the oscillatory behavior through the precession of neutron spin *S* in the local magnetic induction ***B***. The amplitude *B* and the angle θ are reflected in the oscillatory polarization data.

The neutron depolarization measurements were performed using the polarized neutron reflectometer (PORE) spectrometer at the cold neutron guide hall of the Booster Synchrotron Utilization Facility at the High Energy Accelerator Research Organization (Tsukuba, Japan). All the incident neutron spins were polarized along the *z* direction. The polarization $P(\lambda)$ along the *z* direction was measured in a magnetic field *H* as a function of the wavelength λ(2.6 −10.7 Å), using the polarization analyzer just after the neutron passed through the sample along the *x* direction, where the sample plate was parallel to the *yz* plane. The present wavelength resolution ($\Delta\lambda = 0.036$ Å) is four times higher than that in the previous measurements.[12] In the field cooling (FC) procedure, an external field H_{cool} of 1 kOe was applied along the *y* direction, using an electromagnet during the sample cooling to the lowest temperature in the present measurement (~7 K), and the polarization measurement was performed on a heating run. The arrangement of H_{cool} and *H* in the present neutron experiment is described in Fig. 1(a).

The magnetic measurement was performed using a commercial superconducting quantum interference device magnetometer. The magnetic measurement of the spherical sample was performed in a field applied parallel to the direction of H_{cool}. The temperature-dependent magnetization at 20 Oe [Fig. 2(a)] shows a Curie temperature T_C of ~160 K and a reentrant spin-glass temperature T_{RSG} of ~60 K, which

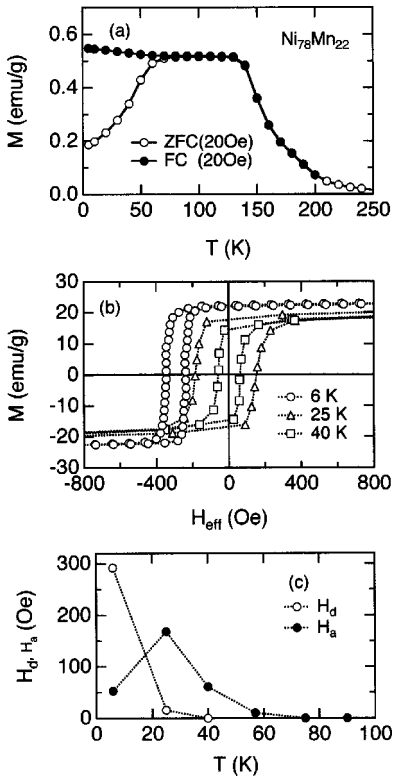

FIG. 2. ZFC and FC values of magnetization of $Ni_{78}Mn_{22}$ measured as a function of temperature in a field of 20 Oe (a). FC magnetization curves at 6, 25, and 40 K are shown in (b), where H_{eff} is the effective field corrected for the demagnetization field. The unidirectional and uniaxial anisotropy fields are evaluated based on the magnetization curves in (c).

values are slightly higher than those of the Ni_{77} $^{57}Fe_1Mn_{22}$ sample used in the previous work ($T_C \sim 150$ K and $T_{\mathrm{RSG}} \sim 50$ K).[9] Nevertheless, we decided to compare the present results of the neutron study with the previous Mössbauer data, based on the fact that the spin-freezing behavior of this system is mainly dependent on the Mn content. The field-dependent magnetization was measured after cooling the sample down to a measuring temperature in a field H_{cool} of 10 kOe, where the measurement was performed in a field applied parallel to H_{cool}. The spontaneous magnetization of 22.4 emu/g and the unidirectional anisotropy field of 290 Oe were obtained at 6 K [Fig. 2(b)], and these values are comparable to those reported by Kouvel, Abdul-Razzaq and Ziq.[15] The low temperature evolution of unidirectional and uniaxial anisotropy fields H_d and H_a is shown in Fig. 2(c). The unidirectional term of anisotropy disappears at temperatures higher than 40 K, and the uniaxial term shows a maximum around 30 K and successively decreases as temperature decreases. These characteristics are consistent with those reported in the reentrant system of NiMn.[16]

In the additional magnetic measurement of the disc sample, a magnetic field was applied perpendicular to the direction of H_{cool} in a manner similar to that used in the neutron measurement; i.e., the sample was rotated 90° using a sample rotator (Quantum Design, California, USA) in a zero field after cooling the sample to the measuring temperature in a field of 1 kOe. In Fig. 3(a), the low-field magnetization curve at 8 K under the 90°-rotation condition is compared with that measured in the conventional way. A small and symmetric hysteresis is observed in the 90°-rotation data, which is in contrast to the asymmetric shape of the conventional data. The magnetization curves were obtained at temperatures which were the same as those of the neutron measurements. The 90°-rotation magnetization, measured at various temperatures, is shown as a function of temperature in Fig. 3(b). As temperature increases, the magnetization rapidly decreases below ~50 K and shows a slow increase followed by a plateau region, and decreases around T_{C}. These data will be directly compared with the neutron data.

III. EXPERIMENTAL RESULTS AND ANLYSIS OF NEUTRON DEPOLARIZATION DATA

Figure 4 shows the typical zero field cooling (ZFC) and FC features of the wavelength-dependent neutron polarization in a field of 90 Oe. At 8 and 40 K($<T_{\mathrm{RSG}}$), thermal irreversibility was significantly observed; oscillatory behavior was seen in the FC data and monotonic decrease in the ZFC data [Figs. 3(a) and 3(b)]. At 65 K ($\sim T_{\mathrm{RSG}}$), the ZFC and FC data similarly show oscillatory behavior [Fig. 3(c)]. At 80 K ($\sim T_{\mathrm{RSG}}$), the oscillatory features observed in the ZFC and FC data, respectively, are intrinsically the same [Fig. 3(d)]. This wavelength dependence, observed just above T_{RSG}, cannot be expressed by a kind of damped oscillation with a unique period. At higher temperatures, the oscillatory behavior contains only one period [Fig. 3(e)]. We will analyze these kinds of wavelength dependence based on the expressions shown in the following paragraph.

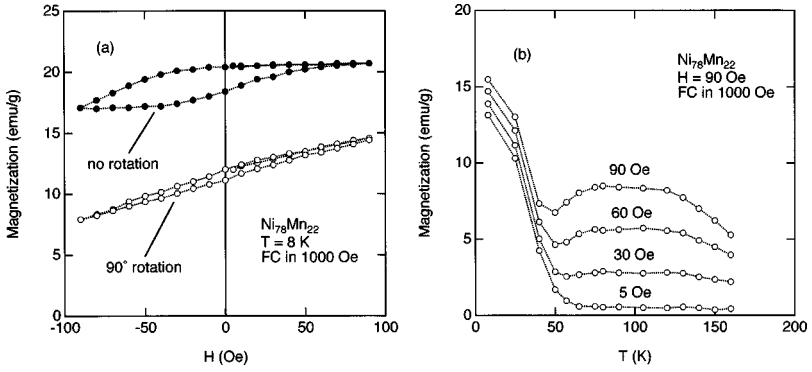

FIG. 3. (a) The magnetization of the plate sample of $Ni_{78}Mn_{22}$ is measured as a function of applied field, where the sample was rotated 90° in a zero field after cooling of the sample to the measuring temperature in a field of 1 kOe. In addition, the magnetization curve under the FC condition with H_{cool} of 1 kOe, measured in a conventional way, is compared with the 90°-rotation data. (b) The FC magnetization, measured under the condition of 90° rotation, is plotted as a function of temperature.

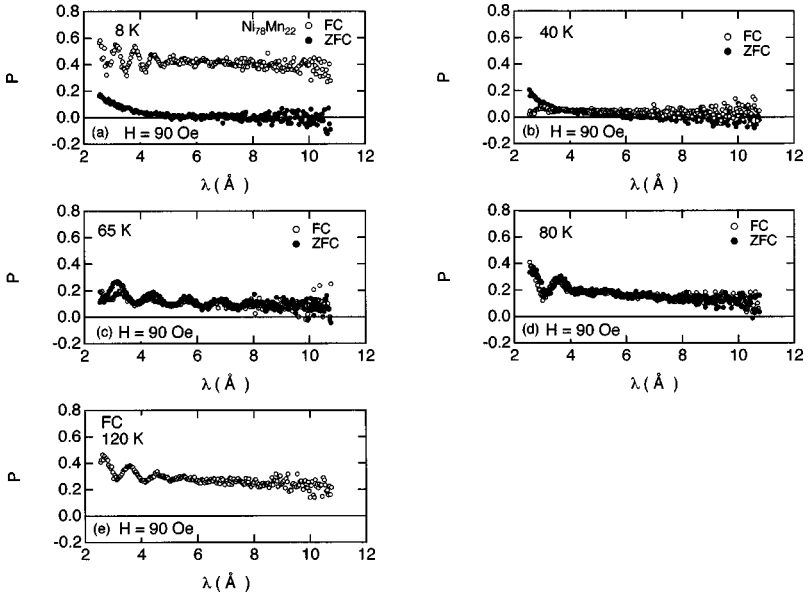

FIG. 4. ZFC and FC features of wavelength-dependent neutron polarization of $Ni_{78}Mn_{22}$, measured in a field of 90 Oe, are shown at 8, 40, 65, 80, and 120 K. At 8 and 40 K ($<T_{RSG}$), the thermal irreversible behavior is observed, but it disappears at high temperatures above 80 K ($>T_{RSG}$). At 65 K ($\sim T_{RSG}$), a marginal behavior is observed.

Mitsuda and Endoh[17] characterized the wavelength-dependent polarization $P(\lambda)$ of a polarized neutron traveling through a magnetic medium based on the classical treatment by Halpern and Holsteinas.[11] The characteristics of $P(\lambda)$ are summarized as follows:

(1) For a large domain limit of the ferromagnet (monodomain structure), a damped oscillatory wavelength dependence, where the damping factor depends on the inhomogeneity of the magnetic induction in the sample, is observed. Figure 1(b) shows the schematic drawing of the oscillatory polarization, which originates from the precession of the neutron spin $\boldsymbol{s}$ induced by the magnetic induction $\boldsymbol{B}$ in a homogeneous ferromagnetic medium. The period of oscillation corresponds to the amplitude of $\boldsymbol{B}$, where $\boldsymbol{B} \sim 4\pi \boldsymbol{M}$ in a small applied field, and the average polarization is determined by the angle θ between $\boldsymbol{B}$ and the z axis. This is useful to characterize the magnetic structure on a semi-macroscopic scale.

(2) For a multidomain state of the ferromagnet, the oscillatory behavior is washed out due to the random orientation of the domains, and an exponential-type monotonic decrease, where the exponent depends on the magnetization and the size of magnetic domain, is observed. In addition, Dokukin *et al.*[18] proposed a modified expression of the wavelength-dependent polarization based on the theory of polarized neutron scattering given by Toperverg and Weniger.[19] The expression contains the fluctuation of magnetic induction parallel to the mean magnetic induction $\langle B \rangle$ in addition to the perpendicular component. Further, Krezhov *et al.*[20] took into account the effect of the width of the neutron pulse, and deduced the following type of expression for the large domain limit under the condition of small distribution of B

$$P(\lambda) = \exp(-c_1\lambda^2)\cos^2\theta + A\,\exp(-c_2\lambda^2)\sin^2\theta\,\cos\,(I\lambda + \phi), \tag{1}$$

and

$$I = C\langle B \rangle L, \tag{2}$$

where c_1 and c_2 are related to the width of distribution of the magnetic induction parallel and are perpendicular to $\langle B \rangle$, respectively. The coefficients A and ϕ depend on the width of the neutron pulse, the neutron flight path, and the sample thickness L. The field integral I, defined by Eq. (2), can be used to determine $\langle B \rangle$, where $C = 4.63 \times 10^2$ cm^{-1} Oe^{-1} Å^{-1}.[17] Based on Eq. (1), we propose the following modified expression applicable to the magnetic medium comprised of two different magnetic regions with different respective magnetic inductions, I_{low} and I_{high}

$$\begin{aligned} P(\lambda) = {} & \exp(-c_1\lambda^2)\cos^2\theta + a\,A\,\exp(-c_1\lambda^2) \\ & \times \sin^2\theta\,\cos(I_{low}\lambda + \phi) + (1-a)A\,\exp(-c_2'\lambda^2) \\ & \times \sin^2\theta\,\cos(I_{high}\lambda + \phi'), \end{aligned} \tag{3}$$

where $a/(1-a)$ is the volume ratio of the two magnetic regions.[21]

Figure 5(a) shows the FC data, obtained in the applied field of 90 Oe at 8 K, that characterizes the wavelength dependence below T_{RSG}. The oscillatory behavior is well expressed by Eq. (1). When the applied field was below 60 Oe, distorted oscillatory behavior was observed, although no such behavior is shown in Fig. 5. This is because the polarized neutron is depolarized, due to the stray field from the sample, prior to coming into the sample. Just above T_{RSG}, the complex wavelength dependence of polarization, as observed at 80 K, appeared [Fig. 5(b)]. This cannot be expressed by Eq. (1), because the best fit based on Eq. (1) brings about unreasonable values of $P(>1)$ at small λ, as shown in the inset of Fig. 6. On the other hand, Eq. (3), which includes two kinds of oscillatory terms, well expresses the complex behavior (Fig. 6). At higher temperatures, Eq. (1) again becomes the suitable expression, as observed at 120 K [Fig. 5(c)]. After all, the wavelength-dependent polarization can be well expressed by the single oscillatory term both in the RSG and FM phases, except in the temperature region just

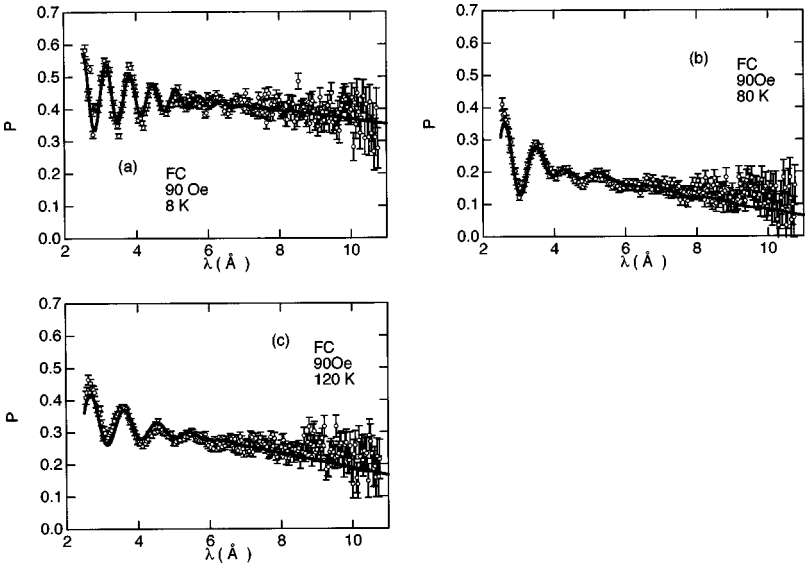

FIG. 5. FC wavelength-dependent neutron polarization of $Ni_{78}Mn_{22}$, measured at 90 Oe, is shown together with the theoretical curves. At 8 and 120 K, Eq. (1) is a good expression, but the double oscillatory behavior is observed at 80 K, which can be expressed by Eq. (3).

above T_{RSG}. Thus, the essential domain structure of the FC-RSG and FM phases in reentrant $Ni_{78}Mn_{22}$ can be interpreted based on the large-scale ferromagnetic domain. However, the sum of the two kinds of oscillatory terms, appearing just above T_{RSG}, is an observation that has not been detected in previous studies. We demonstrate the meaning of the double oscillation by the temperature-dependent behavior of the field integral in the following paragraphs, thereby providing a comprehensive picture of the spin freezing process of the present reentrant ferromagnet.

Figure 7(a) shows the values of I obtained from the FC data at 90 and 60 Oe. In addition, the FC data in a low-field (5 Oe) and the ZFC values, obtained from the data in 90 Oe, are plotted in Fig. 7(b), where the field integral can be observed only around T_{RSG}. The values of I, calculated based on Eq. (2) using the relation $B=4\pi M_s$ (M_s is the spontaneous magnetization deduced by the extrapolation using the high-field magnetization data obtained between 2 and 10 kOe), are shown by the dotted curve in these figures. The FC values of I, obtained at 90 and 60 Oe, agree well with the calculated curve below 40 K. As the temperature increases above 40 K, the value of I deviates downward from the calculated curve. Around 80 K, the lower-value I_{low}, which was deduced from the larger period term in the double oscillatory function, is smoothly connected to the lower-temperature values, and the higher-value I_{high}, corresponding to the shorter period term, is almost the same as the calculated value. At higher temperatures, the value of I monotonically decreases as the temperature increases, and follows along the calculated curve. Therefore, there are two branches in the temperature-dependent values of I, which govern the corresponding two temperature regions, below and above T_{RSG}. The thermal evolution of the FC value of I in 5 Oe, observed in Fig. 7(b), resembles that of I_{low} shown in Fig. 7(a), although oscillatory polarization with a regular period is observed only around T_{RSG}. In addition, the ZFC data show the oscillatory behavior at temperatures higher than 50 K. The temperature-dependent ZFC value of I is similar to that of FC values at 90 and 60 Oe; i.e., the two branches of I are observed just above T_{RSG}. Therefore, the observation of the I_{low} branch is intrinsically independent of both the cooling condition and the amplitude of the applied field, although the I_{high} branch is not observed in a field of 5 Oe. In addition, the low-field polarization, measured at the higher temperatures, shows no oscillatory behavior but does show monotonic decrease. This suggests that a field of 5 Oe is insufficient to generate the monodomain configuration. Thus, the observation of the I_{low} branch is independent of the domain configuration.

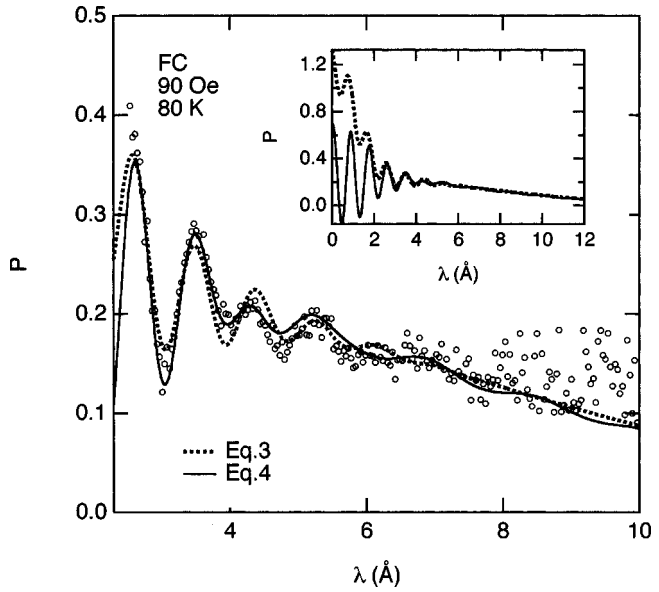

FIG. 6. Based on Eqs. (1) and (3), the best fits to the 80 K data are shown. The fit based on Eq. (3) shows unreasonable behavior at small λ, as shown in the inset.

Next, we evaluated the z component of magnetization M_z based on the values of I and θ, where the value of θ is determined by the first term ($=\cos^2\theta$) in Eq. (1) because the second term includes an ambiguous parameter A.[22] In Fig. 7(c), the temperature-dependent values of M_z are compared with the magnetization obtained by the magnetic measurement in the 90°-rotation procedure, where the double oscil-

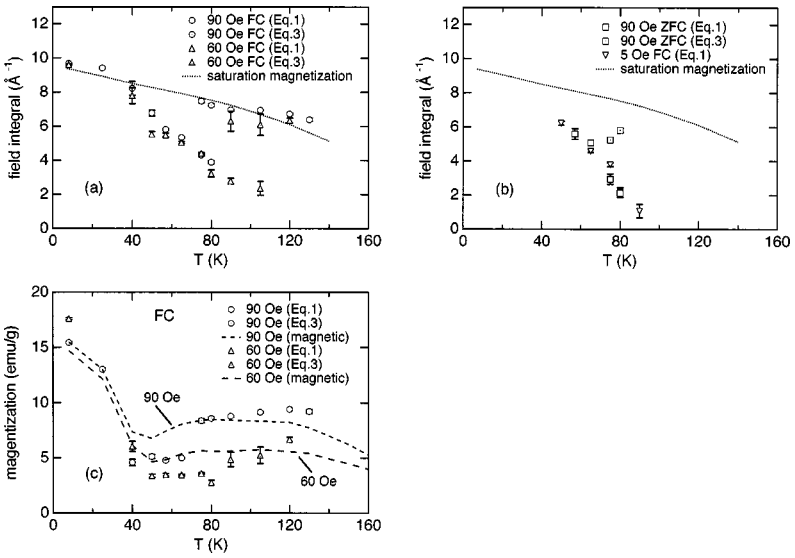

FIG. 7. Temperature dependence of the FC field integral I of $Ni_{78}Mn_{22}$, evaluated at 90 and 60 Oe, is shown in (a). The FC values of I obtained at 5 Oe and the ZFC values of I obtained at 90 Oe are plotted as a function of temperature in (b). The calculated curve, obtained based on the magnetization data measured at magnetic fields between 2 and 10 kOe, is shown as a dotted curve in both figures. The z components of magnetization, evaluated from I and θ obtained in the 90 and 60 Oe, are compared with the magnetic data (dashed curves) in (c).

latory data is analyzed in consideration of the volume ratio of two magnetic regions. The two sets of data are intrinsically identical in the temperature regions below 40 K and above 80 K, but the value of M_z, obtained based on the neutron data, is significantly smaller than the magnetic data around T_{RSG}. This suggests that a portion of the spins do not belong to the large magnetic domain corresponding to the oscillatory polarization; i.e., the multidomain structure is partly formed under the FC condition at temperatures around T_{RSG}.

IV. DISCUSSION

At temperatures lower than 40 K, the amplitude and z component of magnetization evaluated based on the FC neutron depolarization data essentially agree with the magnetic data measured under the same conditions used for the neutron measurement. This finding is consistent with those in the previous study of the Mössbauer effect and ac susceptibility of $Ni_{77}Fe_1Mn_{22}$, indicating that spin-glass ordering homogeneously coexists with long-range ferromagnetic correlation in the RSG phase. Now we discuss the reason why the large z component of magnetization is observed despite the FC procedure in a field of 1 kOe along the y direction, i.e., why the net magnetization vector significantly cants from the direction of H_{cool}. A similar situation has been observed in previous studies of the reentrant NiMn system based on the neutron depolarization experiment and the transverse ac susceptibility measurement. This has been interpreted in terms

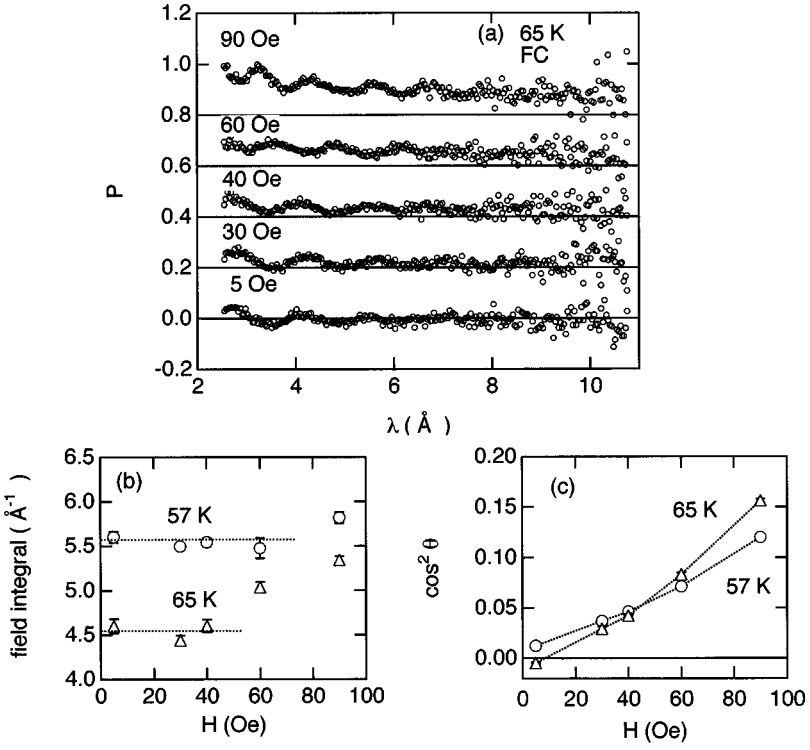

FIG. 8. The FC feature of wavelength-dependent neutron polarization of $Ni_{78}Mn_{22}$ measured at 65 K in various magnetic fields below 90 Oe is shown in (a). The values of the field integral and $\cos^2\theta$, deduced from the FC data measured at 57 and 65 K, are plotted as a function of the applied field in (b) and (c).

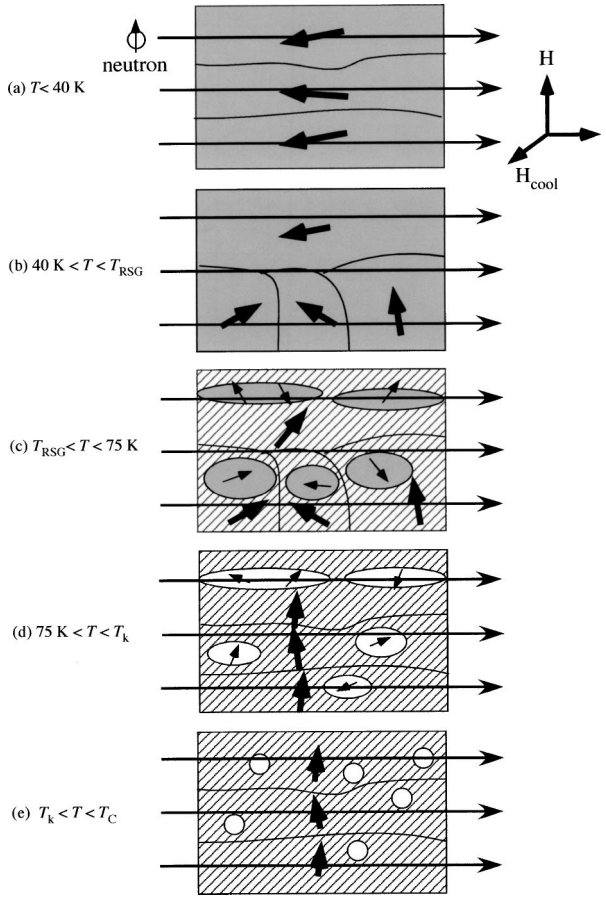

FIG. 9. The spin freezing process in reentrant ferromagnet $Ni_{78}Mn_{22}$ after the FC procedure, schematically summarized. The temperature range is classified into five groups: (a) $T<40$ K, (b) 40 K$<T<T_{RSG}$, (c) $T_{RSG}<T<75$ K, (d) 75 K$<T<T_k$, and (e) $T_k<T<T_C$. The gray and hatched regions represent the canted and collinear aligned spins in (a)–(c), respectively. The white region represents the fluctuating spins around the frustrated spin site in (d) and (e). A detailed explanation is given in the text.

of the domain reorientation induced in the process of decrease in magnetic field after the FC procedure. Thus, we can estimate the resultant monodomain structure that consists of domains having a magnetization vector canting from the y direction. This structure should be determined by four kinds of terms: the effective field H_{eff} determined by the applied field and demagnetization field, the unidirectional anisotropy field H_d, the uniaxial anisotropy field H_a, and the effective exchange field H_{ex} of coupling between adjacent domains.

In the temperature region of 50–75 K, the field integral deviates downward from the magnetic data where there is a difference between the values of M_z and the magnetization data. This is followed by the double oscillatory behavior above 75 K. This characteristic behavior can be interpreted based on both the change in the domain configuration and the change in spin configuration in a domain.

As mentioned in the previous work using Mössbauer measurement, there are two kinds of distributions of the hyperfine field in the ferromagnetic region, which were assigned to the spins with long and short relaxation times, respectively. This distribution can be related to the double oscillatory behavior of neutron depolarization. In the temperature range between 50 and 75 K, however, only the I_{low} branch is observed. In this region, the multi-domain structure is partly formed as mentioned above. This washes out the oscillatory behavior originating from the collinear spins with long relaxation time. Thus, the I_{high} branch disappears. At temperatures above 75 K, the application of magnetic field easily induces the monodomain structure due to the low coercive field ($<$10 Oe), and the contribution from the collinear spins reappears as the oscillatory polarization. This results in observation of the I_{high} branch. On the other hand, the I_{low} branch can be explained based on the spins with short relaxation times, which locate around the frustrated spin sites. Provided the reduction of frustrated spin length is faster than that of the average spin length at temperatures above 50 K, the thermal fluctuation of spins around the frustrated spin site becomes remarkable. When the fluctuated spins combine into a macroscopic magnetic region, the local magnetic induction in this region becomes small compared with that of the collinear spins. Thus, the field integral deviates downward from the evaluated value based on the magnetic measurement. As the temperature further increases, the spin length at the frustrated spin site becomes very short and the melting of frustrated spin is brought about as expected, based on the simulation study by Saslow and Parker.[10] In this situation, the spins around the frustrated spin site fluctuate severely and the collinear spin component is thereby lost. Therefore, I_{low} decreases with increasing temperature toward zero at a temperature T_k below T_C.[23]

The local spin configuration around the frustrated site is sensitively modified by application of magnetic field as demonstrated by the systematic field dependence of wavelength-dependent polarization measured at 65 K [Fig. 8(a)]. The field integral I_{low}, obtained at 57 and 65 K, increases as the magnetic field increases [Fig. 8(b)] except in the low-field region. This explains the field dependence of the I_{low} branch, as shown in Fig. 7. In addition, the value of $\cos^2\theta$ also increases with increasing magnetic field, where it starts from $\sim$0 at $H=0$ [Fig. 8(c)]. This indicates that the spin around the frustrated spin site roughly lies along the y direction in a zero field, and as the magnetic field increases, it turns toward the z direction accompanied by an increase in spin length.

At temperatures between T_k and T_C, the length of ferromagnetic spins is so short the region of frustrated spins becomes microscopic and scarcely contributes to the neutron polarization. Thus, only the I_{high} branch is observed along the temperature-dependent spontaneous magnetization.

We can schematically summarize the spin freezing process after the FC procedure in Fig. 9.

(1) At temperatures below 40 K, the spin-glass order coexists with the long-range ferromagnetic correlation in the monodomain structure.

(2) At temperatures between 40 K and T_{RSG}($\sim$60 K), the multidomain structure, in which spin-glass order coexists with the long-range ferromagnetic correlation, is partially formed.

(3) At temperatures between T_{RSG} and 75 K, the multidomain structure, consisting of the collinearly aligned spins, is formed. In a domain, the long-range spin-glass correlation replaces the finite and macroscopic magnetic clusters con-

sisting of canted spins, which are located around the frustrated spin site. Thus, two kinds of magnetic regions, one with large and one with small magnetic inductions, coexist.

(4) At temperatures between 75 K and T_k, the monodomain structure is easily formed in a magnetic field used in the present work. The spins, located around the frustrated site, fluctuated severely, and therefore have a very small magnetic induction.

(5) At temperatures between T_k and T_C, the frustrated spins melt and the length of the collinear spins becomes very short. Thus, the canting of spin around the melted spin is significantly suppressed and the corresponding region becomes microscopic. As a result, because of the semimacroscopic spatial resolution of neutron measurement, the neutron spin only responds to the average magnetic induction in the sample. In contrast to this, Mössbauer measurement, due to its atomic scale resolution, separately observes the two magnetic regions. This results in the appearance of two peaks in the distribution of the hyperfine field.[9]

This picture of the spin freezing process of reentrant NiMn is consistent with the idea of melting of frustrated spins, which was proposed for XY-type reentrant spin-glass. However, the present work showed no trace of singularity in temperature-dependent magnetization due to spin canting. This is consistent with findings from the simulation study for the frustrated Heisenberg system[24] rather than with the expectation set out by Saslow and Parker. Nevertheless, based on the comprehensive work using some experimental methods with different special resolutions ranging from the atomic to macroscopic scale, we claim that the semimacroscopic inhomogeneity plays an important role in the spin freezing in the reentrant spin-glass.

Finally, we explain the difference in the temperature-dependent behavior of the field integral between the present and previous depolarization measurements. This can be interpreted based on the difference of resolution between the apparatuses presently and previously used. The present measurement, whose resolution is four-times higher than that in the previous work, can reveal the detailed structure of wavelength-dependent polarization, which has not been detected in any previous work. Therefore, we conclude that the two-stage change observed in the previous work is the coarse observation of intrinsic behavior of the field integral.

V. CONCLUSION

The reentrant spin-glass behavior of $Ni_{78}Mn_{22}$, observed in the Mössbauer measurements and neutron depolarization analysis, was persuasively interpreted based on the mechanisms of low temperature spin canting and melting of frustrated spins. We successfully propose a comprehensive picture of the spin freezing process and the magnetic nature of the RSG and FM phases in the typical reentrant ferromagnet. The picture is consistent with finding from the simulation study by Saslow and Parker, except for the absence of singularity in the temperature-dependent magnetization. We note that the anisotropic nature of the NiMn system, which originates from the Dzyaloshinsky-Moriya-type interaction, plays an important role in the spin freezing process in addition to its role in the semimacroscopic inhomogeneity. A neutron depolarization study of a reentrant ferromagnet having the magnetic anisotropy with a different amplitude is planned in the near future.

ACKNOWLEDGMENTS

One of the authors (T.S.) would like to thank Dr. Petra Jönsson and Dr. Roland Mathieu of Tokyo University for their help in performing the magnetization measurement using a sample rotator. This work was performed in FY 2002 The 21st Century COE Program. Financial support from the Fukuzawa Foundation of Keio University is also gratefully acknowledged.

*Present address: Japan Atomic Energy Research Institute, 2-4 Shirane, Tokai-mura, Naka-gun, Ibaraki-ken 319-1195, Japan.

[1] See, e.g., K. Binder and A. P. Young, Rev. Mod. Phys. **58**, 801 (1986); K. H. Fischer and J. Hertz, *Spin-glasses* (Cambridge University Press, Cambridge, 1991); J. A. Mydosh, *Spin-glasses* (Taylor & Francis, London, Washington, DC, 1993).

[2] D. Sherrington and S. Kirkpatrick, Phys. Rev. Lett. **35**, 1792 (1975).

[3] M. Gabay and G. Toulouse, Phys. Rev. Lett. **47**, 201 (1981).

[4] I. Mirebeau, S. Itoh, S. Mitsuda, T. Watanabe, Y. Endoh, M. Hennion, and R. Papoular, Phys. Rev. B **41**, 11 405 (1990).

[5] H. Maletta, G. Aeppli, and S. M. Shapiro, Phys. Rev. Lett. **48**, 1490 (1982).

[6] K. Jonason, J. Mattsson, and P. Nordblad, Phys. Rev. B **53**, 6507 (1996).

[7] K. Jonason and P. Nordblad, J. Magn. Magn. Mater. **177-181**, 95 (1998).

[8] K. Jonason, J. Mattson, and P. Nordblad, Phys. Rev. Lett. **77**, 2562 (1996).

[9] T. Sato, T. Ando, T. Ogawa, S. Morimoto, and A. Ito, Phys. Rev. B **64**, 184432 (2001).

[10] W. M. Saslow and G. N. Parker, Phys. Rev. Lett. **56**, 1074 (1986).

[11] O. Halpern and T. Holstein, Phys. Rev. **59**, 960 (1941).

[12] T. Sato, T. Ando, T. Watanabe, S. Itoh, and Y. Endoh, J. Magn. Magn. Mater. **104-107**, 1625 (1992); T. Sato, T. Ando, T. Watanabe, S. Itoh, Y. Endoh, and M. Furusaka, Phys. Rev. B **48**, 6074 (1993).

[13] J. S. Kouvel and W. Abdul-Razzaq, J. Magn. Magn. Mater. **53**, 139 (1985).

[14] See, e.g., S. Mitsuda, H. Yoshizawa, T. Watanabe, S. Itoh, Y. Endoh, and I. Mirebeau, J. Phys. Soc. Jpn. **60**, 1721 (1991).

[15] S. Kouvel, W. Abdul-Razzaq, and Kh. Ziq, Phys. Rev. B **35**, 1768 (1987).

[16] S. Senoussi, J. Physiol. Paris **45**, 315 (1984).

[17] S. Mitsuda and Y. Endoh, J. Phys. Soc. Jpn. **54**, 1570 (1985).

[18] E. B. Dokukin, D. A. Korneev, W. Loebner, V. V. Pasjuk, A. V. Petrenko, and H. Rzany, J. Phys. Colloq. **49**, C8 2073 (1988).
[19] B. P. Toperverg and J. Weniger, Z. Phys. B: Condens. Matter **71**, 95 (1988).
[20] K. Krezhov, V. Lilkov, P. Konstantinov, and D. Korneev, J. Phys.: Condens. Matter **5**, 9277 (1993).
[21] In Eq. (1), the angles between the magnetization vector and the z axis are approximately expressed using θ common between the two ferromagnetic regions. In the temperature range suitable for Eq. (1), the volume of one region was much larger than that of the other region. Thus, the evaluated value of θ essentially corresponds to the angle for the larger magnetic region. Nevertheless, the values of the field integral can be precisely evaluated for the two magnetic regions because they are obtained from the period of oscillatory polarization.
[22] In the temperature regions below 40 K and above 90 K, the value of A is evaluated to be $\sim$0.37 independent of temperature. In the other temperature region, the complex domain structure makes it difficult to deduce the value of A by the fitting procedure.
[23] We evaluated T_k ranging from 100 to 120 K under the application of magnetic fields of 5–90 Oe. Findings demonstrated that the corresponding spin configuration is sensitively dependent on the application of magnetic field as mentioned in the text.
[24] J. R. Thomson, Hong Guo, D. Ryan, M. J. Zuckennann, and Martin Grant, Phys. Rev. B **45**, 3129 (1992).